

Impact Study of Isolated and Correlated Manufacturing Tolerances of a Permanent Magnet Synchronous Machine for Traction Drives

Christoph Mülder
Institute of Electrical Machines (IEM)
 RWTH Aachen University, Germany
 cm@iem.rwth-aachen.de

Marius Franck
Institute of Electrical Machines (IEM)
 RWTH Aachen University, Germany
 mf@iem.rwth-aachen.de

Michael Schröder
Institute of Electrical Machines (IEM)
 RWTH Aachen University, Germany
 ms@iem.rwth-aachen.de

Markus Balluff
Daimler AG
 Stuttgart, Germany
 markus.balluff@daimler.com

Andreas Wanke
Daimler AG
 Stuttgart, Germany
 andreas.wanke@daimler.com

Kay Hameyer
Institute of Electrical Machines (IEM)
 RWTH Aachen University, Germany
 kh@iem.rwth-aachen.de

Abstract— In the course of a growing market share of electrified vehicles, electrical machines will be manufactured in a large scale. The production of high quantities leads to a scattering of the final geometries of e.g. the electrical steel sheets or bearing arrangements. Additionally, the dimensions, mountings and magnetic properties of permanent magnets are subjected to tolerances. This affects both, the electromagnetic and mechanical properties, as well as the acoustic behavior of the machines and therefore the operational behavior of the electrical drive in terms of acoustic emission and driving ability. For the initial analysis, finite-element simulation models are used to take non-linearities, e.g. saturation effects, into account. The purpose of this work is to analyze on the one hand the impact of correlated tolerances to identify tolerance combinations that enhance or weaken each other. On the other hand, isolated tolerances are studied to evaluate the impact on the considered target quantity. Random distributed asymmetric tolerances and eccentricities are simulated based on the tolerance analysis.

Keywords— Acoustic emission, numerical models, electromagnetic, electromagnetic fields, electromagnetic forces, magnetic flux density, manufacturing, permanent magnet machines, tolerance analysis

I. INTRODUCTION

While being assumed to be set up ideal in the computational design process of electrical machines, the manufacturing of electrical machines is always prone to tolerances. Due to various sensitivities of the operational behavior, it is essential to know the impact of manufacturing tolerances on both, the electromagnetic and mechanical properties, e.g. mechanical torque and power, in the following called “performance” and the noise, vibration and harshness (NVH) behavior. Since the two mentioned aspects are immediately experienced by the driver, the designer of electrical traction drives needs to know the interdependencies of such key parameters, already at an early design stage. In [1], the impact of manufacturing tolerances on cogging torque is studied separating rotor and stator parameter tolerances. Since radial force excitations are important in terms of acoustic behavior, the sensitivity should also be considered in this work. Both, the torque and the radial forces with its fundamental and harmonic waves acting in the machine can be derived from the complex air gap flux density

waveform $\underline{B}_\delta(\alpha, t)$ with its spatial dependency α and time dependency t respectively. The field solution can be obtained analytically or numerically. Due to its high computing speed and the possibility to investigate the relationship between cause and effect, the analytical approach of conformal mapping is set out in [2], where the complex flux density is separated according to

$$\underline{B}(\alpha, t) = B_{\text{rad}}(\alpha, t) + j B_{\text{tan}}(\alpha, t) \quad (1)$$

with the radial flux density component B_{rad} and tangential component B_{tan} respectively.

The authors used the method to study equally manufacturing tolerances, e.g. eccentricities, in the case of a surface mounted permanent magnet machine, though concluded that the results are more accurate for the radial than for the tangential component.

The identified orders matched with the finite element simulation that uses the same set of equations to calculate the electromagnetic excited forces. Based on the flux density solution the radial force density

$$\begin{aligned} \sigma_{\text{rad}}(\alpha, t) &= \frac{1}{2\mu_0} (B_{\text{rad}}^2(\alpha, t) - B_{\text{tan}}^2(\alpha, t)) \\ &\approx \frac{1}{2\mu_0} B_{\text{rad}}^2(\alpha, t) \end{aligned} \quad (2)$$

and the tangential force density

$$\sigma_{\text{tan}}(\alpha, t) = \frac{1}{\mu_0} B_{\text{rad}}(\alpha, t) B_{\text{tan}}(\alpha, t) \quad (3)$$

representing analogically real and imaginary part of the complex force density $\underline{\sigma}(\alpha, t)$ and can be obtained with help of the Maxwell stress tensor. μ_0 is the vacuum permeability. The approximation in (2) is made, since the magnetic flux runs predominately in radial direction in the air gap. The corresponding flux density component is much higher than that in tangential direction.

The integral of the tangential force density (3) assumed to be invariant in axial direction, which is sufficient for radial field electrical machines, yields the mechanical torque

$$M(t) = r^2 l \int_0^{2\pi} \sigma_{\tan}(\alpha, t) d\alpha, \quad (4)$$

where r is the air gap radius and l is the axial active length of the machine.

The stated theoretical framework is universal applicable, independently of whether analytical or numerical calculation methods are used to determine the field solution in (1). In the course of this work, a numerical field calculation method, the finite element simulation is used. The relation between e.g. the radial force density waves and tooth forces is derived in [3] based on the spatial and temporal Fourier decomposition of (2) and (3) yielding to

$$\sigma(v, f) = \sum_k \sum_l \sigma_{k,l} \cos(v_k \alpha + \omega_l t - \phi_k), \quad (5)$$

where $\sigma_{k,l}$ is the amplitude of the k -th spatial and l -th temporal force density wave, v_k the k -th spatial order, ω_l the l -th frequency order, t the time, f the frequency and ϕ_k the phase-shift angle of the k -th ordinal number. The radial force experienced by a tooth with index i is consequently given by

$$F_{\text{rad}}(i) = 2\pi lr \sum_k \frac{\sin\left(\frac{v_k b_z}{2}\right)}{v_k} \sigma_{\text{rad},(k,l)} \cdot \cos\left(v_k(i-1)\frac{2\pi}{N_1} + \omega_l t - \phi_k\right), \quad (6)$$

where N_1 is the number of stator teeth and b_z the tooth tip width.

The authors conclude that the amplification factor, the first term after the sum sign, is reciprocally proportional to the ordinal number v_k . Thus, the force excitation decreases analogy considering the mechanical transfer path.

For the tooth force calculation based on finite element simulation, an approach is proposed in [4]. The authors state that the averaged tooth sum force related to a point of force application can be calculated by the nodal forces along the tooth contour, the solution domain e , to

$$F_{\text{rad,avg}}(i) = \sum_{n \in e} F_{\text{rad}}(n), \quad (7)$$

where F_{rad} is the radial force component of the node n . Comparing (6) and (7) leads to the dependency of the nodes in the finite element mesh and the spatial ordinal number v_k . Thus, the finite element model must be discretized carefully, e.g. with enough nodes, when evaluating high orders k in (6).

In this work, various magnet and tooth geometry parameters with tolerances as well as eccentricities are studied

by finite element simulations, to analyze the impact on both, the tangential force density corresponding to the torque and the radial force density. Particularly, the radial tooth force amplitude of one ordinal number is studied in detail since it has been identified experimentally as a critical noise excitation order. After the description of the studied machine and tolerances (modeling), the results of different design points (DPs) in the simulation of correlated and isolated tolerance parameters are discussed. Afterwards, results for asymmetric tolerances and eccentricities are shown. The structure of this work according to the flow chart of the impact study is depicted in Fig. 1. At the end of this work, the results are concluded, and further studies are motivated.

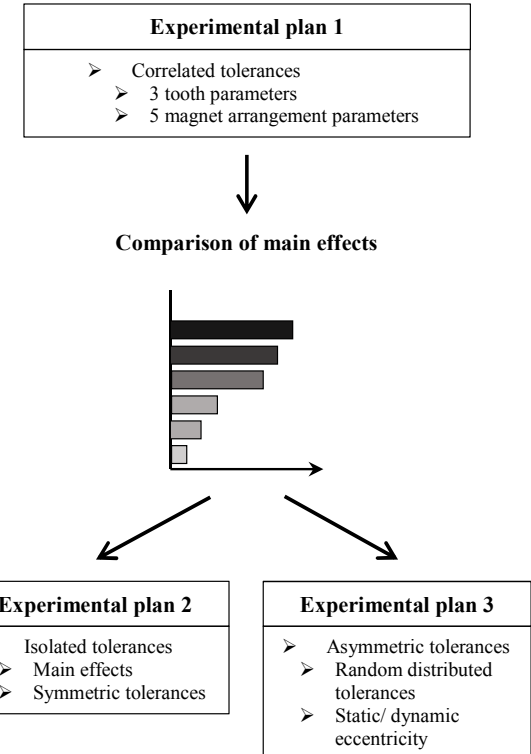


Fig. 1. Flow chart of tolerance impact study.

II. MODELING

In TABLE I, the data of the studied machine for a traction drive is listed. For the simulation of the tolerances and eccentricities a fully parametrizable finite element 2D-model has been built up.

TABLE I. MACHINE DATA.

Quantity	Symbol	Value	Unit
Rated power	P_N	80	kW
Max. phase current	$I_{S,\max}$	450	A
Max. speed	n_{\max}	6400	rpm
Number of stator slots	N_S	30	–
Number of pole pairs	$2p$	20	–
Number of phases	m	3	–
Air gap width	δ	1	mm

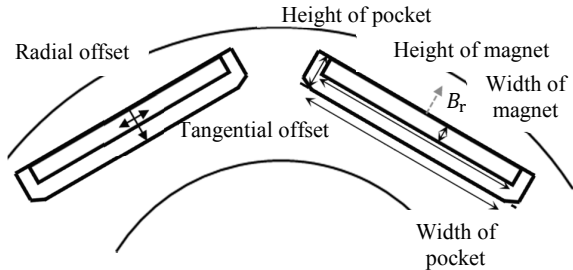


Fig. 2. Schematic illustration of studied parameters of magnet arrangement with tolerances.

For symmetrical (and correlated) tolerances, a sectional model of one pole pair has been used. In the second step, asymmetric tolerances and eccentricities have been analyzed by the full model. In Fig. 2 and Fig. 3, the studied manufacturing tolerances are illustrated schematically. In total, three stator tooth parameters, three magnet parameters, two magnet pocket parameters as well as two magnet position parameters have been studied.

In Fig. 4, a schematic illustration of static and dynamic eccentricity is shown to point out the difference and implementation in finite element simulation. While in the case of static eccentricity, the rotor including the axis of rotation is displaced relative to the center of the stator bore, in the case of dynamic eccentricity the rotor rotational axis is concentric with the stator. As a result, the rotor does not assume a fixed position in the stator bore and the change in the air gap width caused by the dynamic eccentricity rotates in time dependent.

In the first experimental plan, 128 designs subjected to tolerances and the nominal model (design point 0) were simulated with different cross-correlations of the shown parameters. Therefore, peak performance parameters, e.g. maximum torque and power, were calculated by variable control tables in terms of I_d - I_q -current combinations. For the analysis of radial tooth force excitations, three chosen operational points in the speed-torque-map, that are indicated in Fig. 5 with constant current excitations extracted from the nominal design machine, are studied exemplary. The first point is in generative, the second in motor and the third in no/load operating range. In the following, the described simulation indicators are used for all experimental plans.

A section model is used for the symmetrical and correlated tolerances while a full model is used for asymmetric tolerances and eccentricities. In the next section, the simulation results for the first two explained correlated and isolated tolerance parameter setup in terms of both, performance and acoustic behavior are shown.

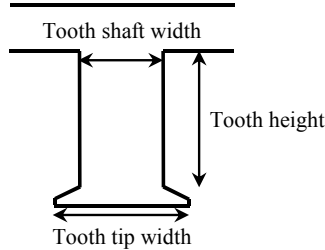


Fig. 3. Schematic illustration of studied tooth parameters with tolerances.

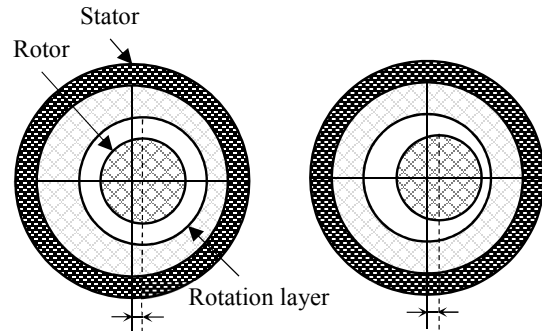


Fig. 4. Schematic illustration of static and dynamic eccentricity for the finite element simulation.

III. SIMULATION RESULTS

A. Correlated tolerances

In the first plan, correlated tolerances have been studied to identify on the one hand the main effects and on the other hand interdependencies in terms of performance and acoustic behavior of the machine. In Fig. 6, the main effect diagrams of selected correlated manufacturing tolerances for the maximum torque are plotted exemplary. The maximum torque deviates for the 128 studied designs in average by approximately 4.1 % from the nominal machine which is indicated by the dashed grey line. It can be observed that the radial offset of a magnet in the pocket has the lowest impact. In contrast to this, the magnet height and particularly the remanence flux density have large impact, since the air gap field is directly correlated to these parameters. The stator tooth height has the largest impact because of the dependency of the air gap width. Considering the results of [5], the press fit of the teeth of a segmented stator can lead to a relative high deflection of single teeth resulting in a local narrowing of the air gap. Therefore, the tolerance in positive direction is much higher than in negative radial direction.

In analogy, the results for the NVH study of the first experimental plan are illustrated in the left plot of Fig. 7. Since the radial tooth force of temporal order $l=60$ has been identified as critical in terms of acoustic radiation, the sensitivity towards manufacturing tolerances have been analyzed in the course of this work. Exemplary, an operational point at approximately rated speed and in partial load is studied (operating point no. 3, cf. Fig. 5). A high scattering of the normalized tooth force amplitude can be observed. Consequently, there are several correlated tolerances with an amplifying and mitigating effect. Particularly, a combination of the three tolerance parameters with the highest impact, as indicated in the performance study, shows a high impact in terms of acoustic behavior. Some points in Fig. 7 indicating the correlation of tolerances should be highlighted without referring to all combinations. The maximum relative deviation in DP 90 is reached by the correlation of lengthening of the stator teeth (resulting in a decrease of the air gap width by about 50 %), increase of both, magnet height and remanence flux density.

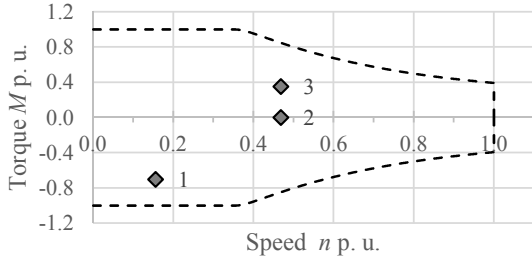


Fig. 5. Peak performance lines of studied machine and operating points of tooth force analysis.

TABLE II. OPERATING POINTS OF TOOTH FORCE ANALYSIS.

Number	Speed p. u.	Torque p. u.
1	0.156	-0.70
2	0.470	0.00
3	0.470	0.35

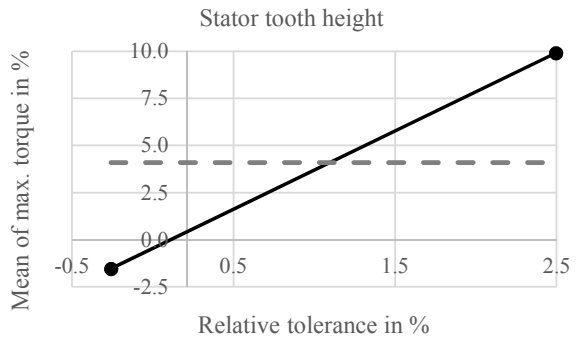
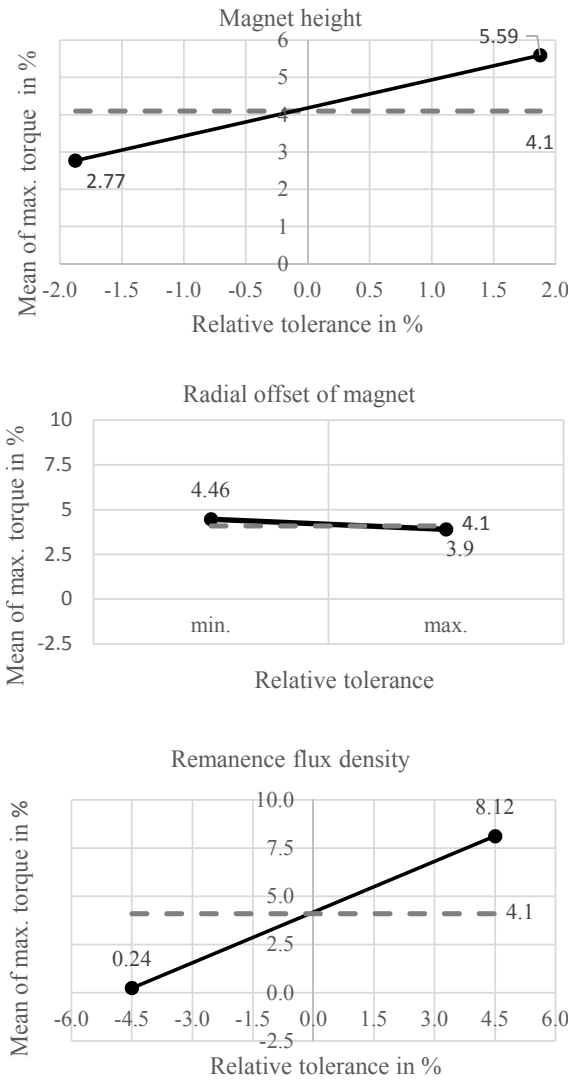


Fig. 6. Main effect diagrams of maximum torque depending on selected manufacturing tolerances of experimental plan 1.

The opposite effect can be identified for the reverse tolerances of the above-mentioned main effect parameters for DP 37 (decrease of tooth height, decrease of remanence and magnet height) that represents the highest negative deviation.

In Fig. 8, the same quantity is illustrated for no-load operation (operating point no. 2). The deviations are in general lower and correlate also to the indicated main effects.

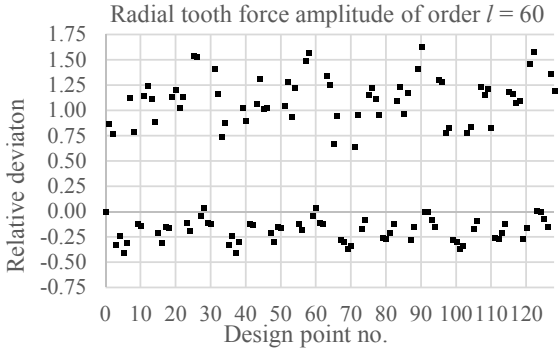


Fig. 7. Relative deviation of radial tooth force amplitude of temporal order 60 of experimental plan 1 design points from reference (DP 0) in operating point no. 3 (motor, partial load).

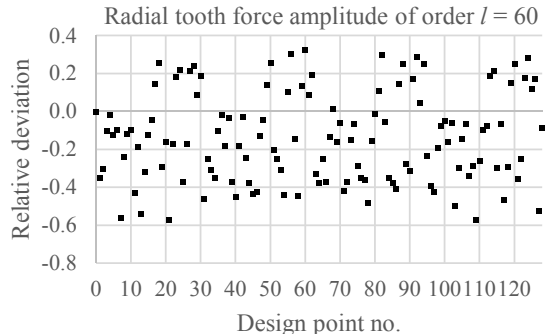


Fig. 8. Relative deviation of radial tooth force amplitude of temporal order 60 of experimental plan 1 design points from reference (DP 0) in operating point no. 2 (no-load).

TABLE III. EXPERIMENTAL PLAN 2.

DP no.	Parameter	Rel. tolerance in %
0	—	—
1	Magnet height	-1.875
2		-0.938
3		0.938
4		1.875
5	Stator tooth height	-0.257
6		-0.129
7		1.236
8		2.472
9	Stator tooth tip width	-0.161
10		-0.081
11		0.081
12		0.161
13	Magnet pocket height	-1.300
14		-0.975
15		-0.650
16		-0.325
17	Radial offset of magnet in pocket	21.739
18		43.478
19		65.217
20		86.957
21	Remanence flux density	-4.500
22		-2.250
23		2.250
24		4.500

pocket). In Fig. 9, the relative deviation of maximum torque from reference (DP 0) is illustrated. As already indicated before, the stator tooth height (design points 5-8) and remanence flux density of the magnets (design points 21-24) have the highest impact, while the other tolerances, as e.g. the magnet pocket height, have only less impact in terms of performance.

In Fig. 10, the relative deviation of the radial tooth force amplitude of temporal order 60 from reference (DP 0) in all studied operating points is shown. Besides the sensitivity towards tolerances in stator tooth height and remanence flux density, a dependency of the operating range can be observed. Particularly for the motor operation point there is a high decrease in the critical tooth force excitation. The remanence flux density has less impact which corresponds to the results of experimental plan 1. The narrowing of the air gap (lengthening of stator tooth) represents the most critical tolerances in terms of force excitation.

C. Asymmetric tolerances

Finally, asymmetric tolerances and static as well as dynamic eccentricities are studied in experimental plan 3, which is listed in TABLE IV. Experimental PLAN 3The full model (complete 2D-cross-section) was used for the finite-element simulation, to be able to distribute tolerances along the whole circumference.

To study the effect of magnet displacements in the pockets, random tilting and translational displacements (in radial and tangential direction) of all magnets were simulated (DP 10 and 11). Design point 1, where all magnets are centered in the pocket, serves as a reference. Design points 12-14 consider tolerances in the remanence flux density for all magnets.

The predominant effects have been studied isolated in the course of experimental plans 2 and 3 therefore depending on the operating range.

B. Isolated tolerances

Based on the identified main effect tolerance parameters, the experimental plan 2, that is listed in TABLE III, was derived. The relative tolerances of the radial offset of the magnets in the pocket (design points 17-20) are related to the maximum possible displacement (bottom space of

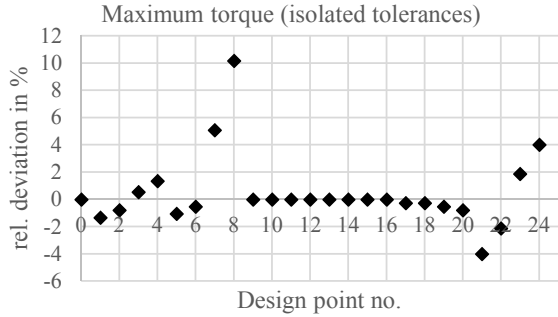


Fig. 9. Relative deviation of maximum torque of experimental plan 2 design points with isolated tolerances from reference (DP 0).

TABLE IV. EXPERIMENTAL PLAN 3.

DP no.	Parameter	Rel. tolerance in %
0	—	—
1	All magnets centered in pocket	—
2	Static eccentricity	10
3		20
4		30
5		40
6		10
7	Dynamic eccentricity	20
8		30
9		40
10	Random displacement of all magnets in pocket	min/max
11	Random tilting of all magnets in pocket	min/max
12	Random distributed remanence deviation	+/- 2.5
13	One magnet magnetized weaker by	-10
14	One magnet magnetized weaker by	-20

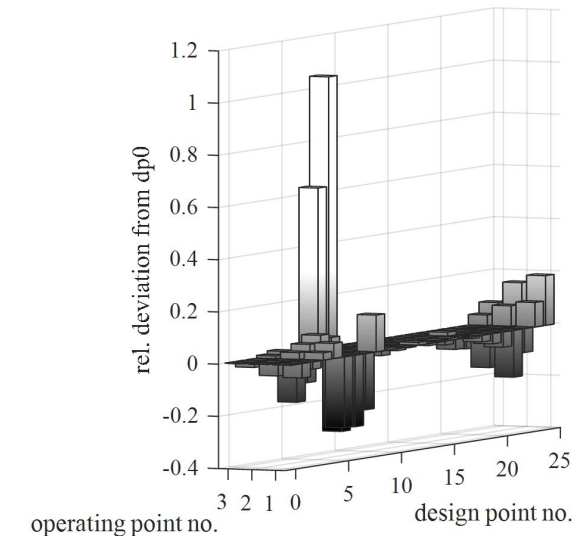


Fig. 10. Relative deviation of radial tooth force amplitude of temporal order 60 of experimental plan 2 design points from reference (DP 0) in all operating points.

In Fig. 11, the relative deviation of maximum torque with isolated tolerances from reference (DP 0) is illustrated. Only slight deviations in terms of maximum performance can be indicated, while all tolerances decrease the torque. The highest mitigation is caused by a separate decrease of remanence of one magnet by 20%. For the other design points, the decrease is under 0.5%.

In Fig. 12, the relative deviation of the radial tooth force amplitude of temporal order 60 from reference at all operating points is shown. Particularly in no-load operation (operating point no. 2), there is a high sensitivity towards asymmetric tolerances. In the other two operating points, the effect is less pronounced. The highest deviation can be observed, when weakening the remanence of one magnet by 20%. This increases the tooth force amplitude by about 12% in no-load operation.

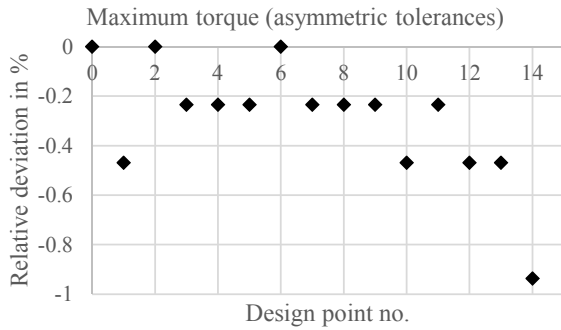


Fig. 11. Relative deviation of maximum torque of experimental plan 3 design points with asymmetric tolerances from reference (DP 0).

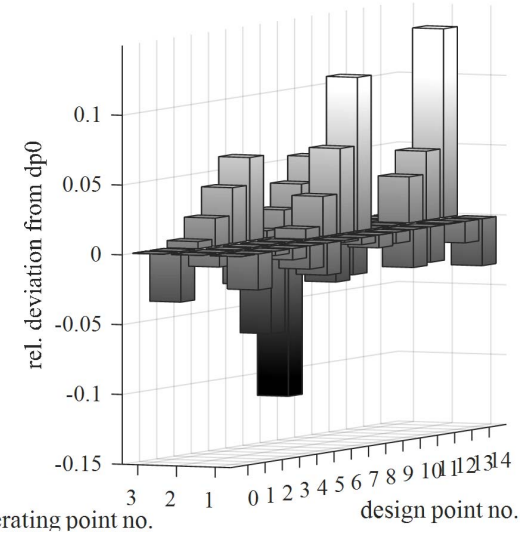


Fig. 12. Relative deviation of radial tooth force amplitude of temporal order 60 of experimental plan 3 design points from reference (DP 0) in all operating points.

IV. CONCLUSIONS

The impact of correlated, isolated and asymmetric tolerances of an electrical machine for a traction drive are studied in this work. Since both, the radial and tangential component of magnetic flux density are influenced by tolerances, performance and NVH behavior are analyzed. Therefore, three stator tooth parameters, two magnet pocket parameters and in total five magnet parameters are considered. The main effect diagrams show that particularly three tolerance parameters have a relevant impact in terms of performance (maximum torque): the stator tooth height, height of the magnets and remanence flux density. This corresponds to the results presented in [1]. Combinations of these parameters show an amplifying effect, related to an acoustic relevant temporal order of a tooth force amplitude. The isolated parameter study shows particularly a sensitivity towards the tooth height or rather air gap width. Moreover, the study shows that the operating range of the machine has additionally influence. Particularly in no-load operation, a high sensitivity towards both, asymmetric magnet variations as well as eccentricity can be observed. The maximum torque is only influenced sparsely by these tolerances.

In conclusion, both, tolerances of stator teeth height, that directly affect the air gap width, as well as magnet tolerances must be carefully considered, since they influence performance and acoustic behavior. Correlated tolerances can enhance each other, so that manufacturing standards must consider these effects.

The force excitations for machines prone to tolerances should evaluated in the whole operating range (drive cycle) or rather in the characteristic diagram in future works. Hereby, the most critical combination of stator current excitations and magnet tolerances can be identified. Additionally, analytical models are considered to compare result with finite element simulations in terms of influence of saturation effects. Further temporal orders of tooth forces will can be considered and combined with structural dynamic aspects to study effects at the drive system level

REFERENCES

- [1] J. Ou, Y. Liu, R. Qu, and M. Doppelbauer, “Experimental and Theoretical Research on Cogging Torque of PM Synchronous Motors Considering Manufacturing Tolerances,” *IEEE Transactions on Industrial Electronics*, vol. 65, no. 5, 2018, pp. 3772–3783.
- [2] M. Schröder, D. Franck, and K. Hameyer, “Analytical modeling of manufacturing tolerances for surface mounted permanent magnet synchronous machines,” in *2015 IEEE International Electric Machines Drives Conference (IEMDC)*, 2015, pp. 1138–1144.
- [3] T. Herold, D. Franck, S. Böhmer, M. Schröder, and K. Hameyer, “Transient simulation model for local force excitations of electrical drives,” *e & i Elektrotechnik und Informationstechnik*, vol. 132, no. 1, 2015, pp. 46–54.
- [4] D. Franck, T. Herold, S. Böhmer, M. Schröder, and K. Hameyer, “Systematic evaluation of vibrational behavior of electric drive trains,” in *2015 Int'l Aegean Conference on Electrical Machines Power Electronics (ACEMP)*, 2015, pp. 1–7.
- [5] M. Balluff, J. Karthaus, M. Schröder, M. Gerlach, and K. Hameyer, “Study on the effects of stator segmentation on the characteristics of an electrical vehicle traction drive,” *ELEKTROTECHNIK UND INFORMATIONSTECHNIK*, vol. 135, no. 2, 2018, pp. 213–222.